

Synthesis and Characterization of Copper Oxide Nanoparticles Synthesized via Chemical Precipitation Method

VeronicaDeekala¹, JyothsnaPragathiYazala¹,Anithakowthalam²,Rameshrajurudraraju^{1*}

1.Department Of Chemistry, Acharya Nagarjuna University, Nagarjuna nagar-522510

2. Department Of Chemistry,Sri Krishnadevaraya University, Ananthapuram-515003

Abstract

The copper oxide nanoparticles were synthesized from copper nitrate trihydrate aqueous solution under the chemical method at 90°C. The average crystallite size was calculated from De-Bye Scherrer's equation. FESEM, EDX, XRD were used to characterize the structure features of the product. FTIR spectra confirmed the adsorption of the copper oxide nanoparticles. In addition, UV-visible absorption spectra were employed to estimate the band gap energy of the copper oxide nanoparticles. This method may be suitable for large scale production of copper oxide nanoparticles for practical applications.

Keywords: Copper oxide, Nanoparticle, Chemical method.

1.1. INTRODUCTION

Nanotechnology gained to a great extent attention for its imperative pioneering role in manipulating materials at the atomic and molecular levels to radically adjust the product properties. Materials reduced to the nanometric scale display significantly different properties compared to what they display at the macroscale or microscales. Because of their unique properties, nanomaterials are widely used in a variety of applications. Small amounts of nanoparticles can play an essential role in developing the properties of materials. Nanoparticles are becoming more and more important day by day as they play a beneficial role in a wide variety of scientific fields. In general, the size of nanoparticles spans the range between 1 and 100 nm. Nanotechnology comprises the design, construction and utilization of functional structures with at least one characteristic dimension measured in nanometres. Currently nanoparticles are widely used in many fields [1-12].

Transition metals are large in number and have number of applications in different field of applications. CuO is one of the useful metal oxide and which has many applications in different fields. Copper oxide nanoparticles are of special interest because of their efficiency as nanofluids in heat transfer applications. It has been reported that 4% addition of CuO improves the thermal conductivity of water by 20% [13-19]. CuO-NPs have been prepared with different sizes and shapes via several methods such as sonochemical [20], direct thermal decomposition [21], electrochemical methods [22], colloid thermal synthesis process [23], and microwave radiation [24]. In the present manuscript, we have synthesized CuO nanoparticles by simple aqueous precipitation method. The copper oxide nanoparticles (CuO-NPs) possess a wide range of applications. Compared with ordinary copper oxide powder, the nano particles of copper oxide show

superior catalytic activity and selectivity. It has excellent antimicrobial activity against various bacterial strains [25]. The CuO-NPs are using in removal of dyes [26]. The CuO-NPs also have an application in heat transfer. Thermal conductivity of CuO based nanofluid is 12.4% higher in comparison with deionised water [27]. This method involves a simple, cheap and one step process for synthesis of CuO nanoparticles.

1.2. Materials and method

1.2.1. Materials

All of chemicals used in experiment are of analytical grade and used as purchased without any purification. Copper nitrate trihydrate ($\text{Cu}(\text{NO}_3)_2 \cdot 3\text{H}_2\text{O}$), of 98% purity is used. De-ionized water used as a solvents. Sodium hydroxide (NaOH) is used to adjust the pH.

1.2.2. Synthesis of copper oxide Nanoparticles

Copper nitrate trihydrate $\text{Cu}(\text{NO}_3)_2 \cdot 3\text{H}_2\text{O}$ and sodium hydroxide NaOH were each dissolved separately in deionized water to form the liquid media of the desired concentrations of 0.05M (12.85g/500mL) and 0.1M (2g/500mL) for sample A and B respectively the ratio of the concentrations was 1:1 ($\text{Cu}(\text{NO}_3)_2 \cdot 3\text{H}_2\text{O}$: NaOH). The copper nitrate trihydrate was slowly added drop- wise to NaOH solutions under vigorous stirring at room temperature, forming transparent white solutions, then inserted into an electrical oven at 90°C for 2 hours. These solutions were reacted to produce copper oxide precipitates. Following the precipitation, the solution was centrifuged at 3000 rpm for 30 minutes. The supernatant was then removed, and the precipitation which contains copper oxide was obtained. Finally, copper oxide was grinded with mortar to be shaped into powder.

1.2.3. CHARACTERISATION

The synthesized copper oxide nanoparticles were characterized by using a UV-DRS in the wavelength range between 200-800 nm. The FT-IR absorption spectra were recorded on a Perkin-Elmer GX FT-IR system used to obtain 16cm^{-1} resolution spectra in the range 400 to 4000cm^{-1} (absorbance mode).

The crystalline structure of the copper oxide nanoparticles were measured by using a Bruker D8 Advance X-ray diffract meter with $\text{CuK}\alpha$ radiation of wavelength $\lambda = 1.54056 \text{ \AA}$. The X-ray diffraction (XRD) measurements were carried out in the locked coupled mode in the 2θ range of 20 to 80.

The surface morphology and composition of copper oxide nanoparticles were investigated by FESEM (Field Emission Scanning Electron Microscopy) developed by Carl Zeiss. An accelerating voltage of 15 to 19 keV and probe current of $\sim 800 \text{ pA}$.

1.3. RESULTS AND DISCUSSIONS

1.3.1. UV Absorption and Reflection Spectra

It was carried out by measuring the diffuse reflectance spectroscopy in UV-Vis range. The spectrum was taken in the range of 200-800 nm. Fig.1 shows the diffused reflectance spectra (absorbance as a function of wavelength). The exciton absorption is at about 260 nm. The optical band gap E_g of the nanoparticles was calculated from Tauc plot as shown in Fig1 the presence of a single slope in the plot suggests that the films have direct and allowed transition. For such transition we have

$$(\alpha h\nu)^2 = A(h\nu - E_g)^n \dots\dots\dots (1)$$

Where α is absorption coefficient, $h\nu$ is photon energy, E_g is optical band gap, n is 1 for direct transition & A is a constant. Fig.2 shows The band gap energy is obtained by extrapolating the straight line portion of the plot to zero absorption coefficient. The band gap value of CuO nanoparticles is found to be 2.26 eV. This red shift of the band gap energy is due to agglomeration of the nanoparticles into larger particles as reported by various authors in different literatures [28-31].

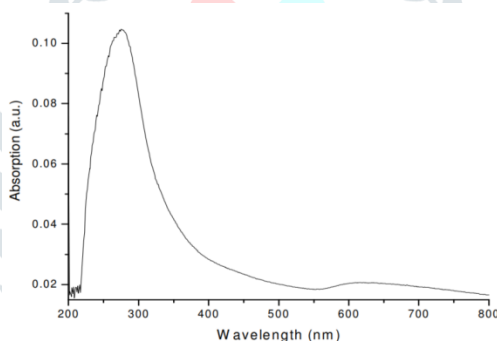


Fig.1: UV-VIS absorption spectrum of as synthesized copper oxide NPs

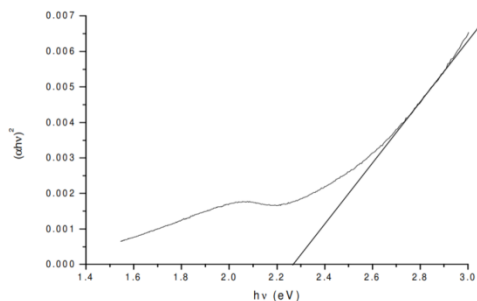


Fig: 2. Tauc plot for as synthesized copper oxide NPs

1.3.2. FTIR Spectrum of copper oxide Nanoparticles

FTIR spectroscopy uses Michelson interferometer to produce an interferogram and the spectrum of CuO is shown in the Fig.3. It has been shown that as particle size decreases, increase in frequency for the bond is observed in nanoparticles. Bands at 416.35 cm^{-1} are assigned to the stretching vibrations of Cu-O. The stretching frequency of bulk CuO is 424 cm^{-1} . Here a blue shift is observed in that frequency i.e., that frequency due to quantum confinement. Three intense bands were centered at 1384.34 cm^{-1} , 1041.54 cm^{-1} and 1556.58 cm^{-1} and are attributed to the stretching vibrations of C = O, C = C and C-H groups in acetate species, which suggests its presents as absorbed species in the surface of nanoparticles. The broad absorption peak centered at 3423.61 cm^{-1} and 1626.40 cm^{-1} corresponds to O-H stretching and bending frequencies of H_2O , indicating the existence of water in the surface of nanoparticles [32]. Variations of the peak positions of CuO [33-35] are presented in the Table 1.

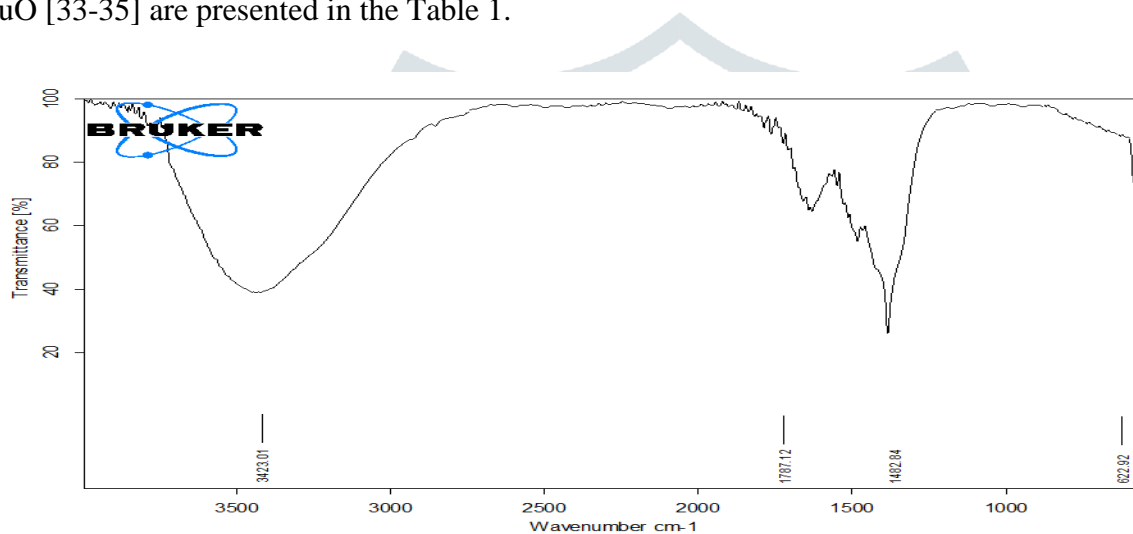


Fig.3 FTIR Spectra of copper oxide nanoparticles

The peak observed at 622.92 cm^{-1} is presence of copper oxide nanoparticle. The broad absorption peak centered at 3423.01 cm^{-1} corresponds to O-H stretching of water indicating the existence of water in the surface of nanoparticles.

S.No	CuO (cm^{-1})	Vibrational modes
1	3423.01	OH
2	1482.84	OH deformation
3	622.92	Stretching of CuO
4	1781.01	C-H

Table.1. Comparison of Vibrational modes of copper oxide nanoparticles

1.3.3. Powder XRD analysis

Fig.4 shows the crystal structure and purity of the synthesized CuO nanoparticles were determined by powder XRD. Fig.4 depicts the xrd pattern of CuO nanoparticles. The prominent diffraction peaks at 2θ values 30.89° , 33.92° , 35.65° , 56.32° , 62.53° , 66.72° , 68.87° , 76.07° are associated with [110], [111], [022], [202], [113], [020], [220], [222] planes respectively. The evolved diffraction peaks could be indexed to a

monoclinic phase of CuO with lattice parameters $a= 4.683 \text{ \AA}$, $b= 3.421 \text{ \AA}$, $c= 5.129 \text{ \AA}$ and corresponds to the JCPDS file no 80-1268. The peak intensities and width of the spectrum indicates the presence of nanoscale crystallites. The absence peaks corresponding to by products such as $\text{Cu}(\text{OH})_2$ or Cu_2O indicate the phase purity of CuO nanoparticles.

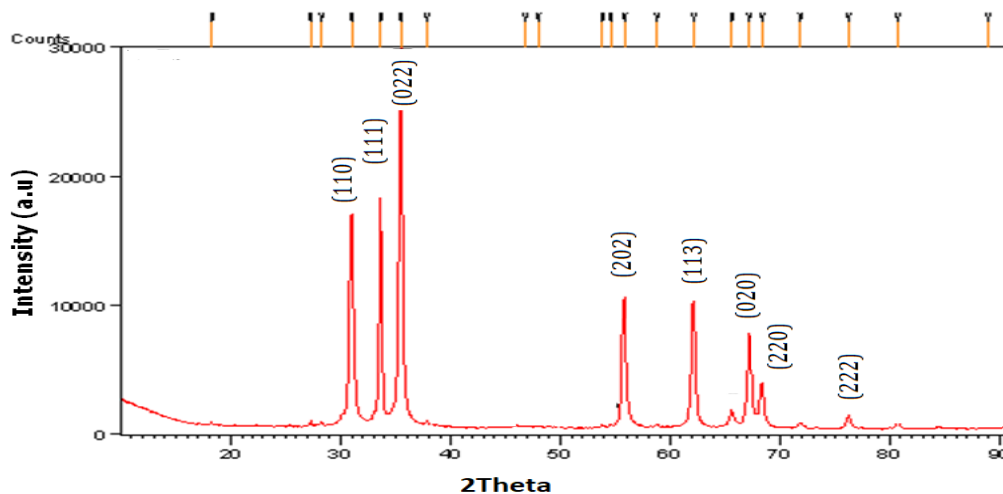


Fig.4. XRD spectra of Copper oxide nanoparticles

2θ	θ	Sinθ	d(Å)	nm	hkl
30.89	15.44	0.266	2.893	77.01	110
33.92	16.96	0.291	2.641	85.02	111
35.65	17.82	0.305	2.517	86.24	022
56.32	28.16	0.471	1.632	73.55	202
62.53	31.26	0.518	1.484	74.93	113
66.72	33.36	0.549	1.401	70.09	020
68.87	34.43	0.565	1.362	65.06	220
76.07	38.03	0.615	1.250	70.92	222

Table.2. d-spacing calculations for copper oxide NPs

Inter planar d-spacing was calculated using Bragg’s Law equation (Table 2):

$$2d\sin\theta = n\lambda \dots\dots\dots (2)$$

where, θ is Bragg’s angle of diffraction, λ is X-ray wavelength, i.e. 1.5406 \AA and $n = 1$. Further, particle size was calculated from the intense peak corresponding to (101) plane using Debye–Scherrer formula. The crystallite size is calculated using Debye Scherrer equation

$$d= 0.9 \lambda / \beta\cos\theta\dots\dots\dots (3)$$

Where d is the average crystallite size (nm), K is the grain shape factor (0.9), λ is the X-ray wavelength (nm), β is the line broadening at half the maximum intensity in radians, and Θ is the Bragg diffraction angle of the 2Θ peak. The average crystallite size was estimated to be 20-50nm.

1.3.4. Field emission Scanning Electron Microscope (FESEM)

FE-SEM image Fig.5. shows the surface morphology and particle size of the synthesized copper oxide nanoparticles. It is clear from the images that the size of the copper oxide nanoparticles is ranging from 20-50 nm. The obtained products are composed of nearly flower shaped morphology with average size in the range of 50 nm.

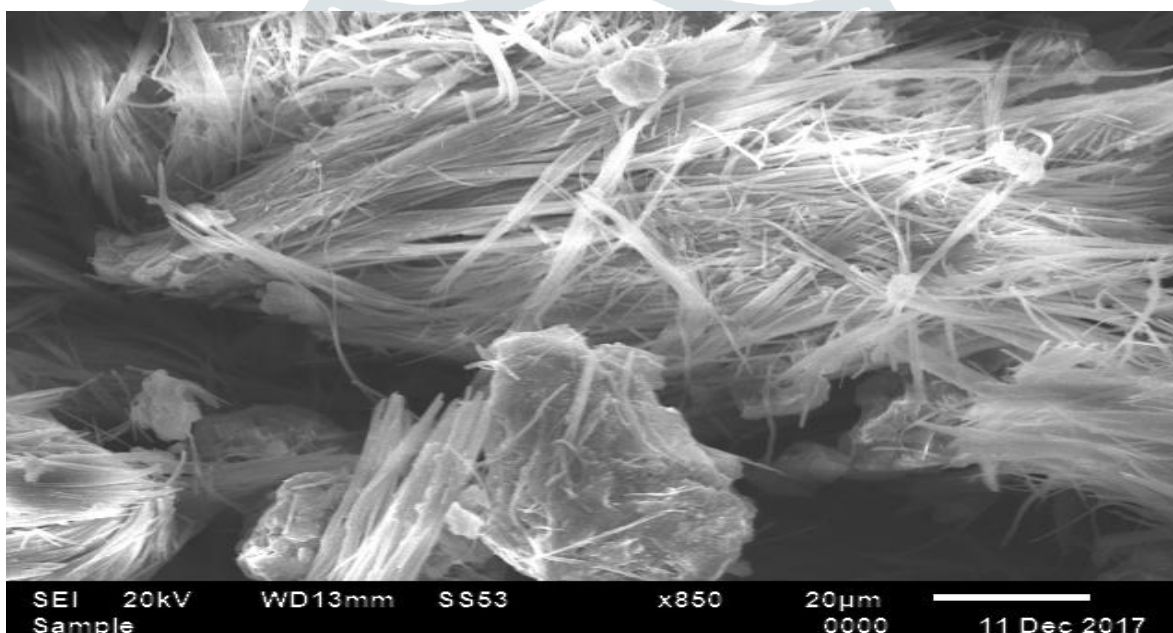


Fig.5. FESEM image of copper oxide nanoparticles

1.3.5. Energy Dispersive X-ray Spectroscopy (EDX)

EDX spectrum, Figure.6, plot not only identifies the elements corresponding to each of its peaks, but the type of X-ray to which it corresponds as well. The higher a peak in a spectrum, the more concentrated the element is in the spectrum. Spherical shaped morphology is observed in the micrograph of copper oxide nanoparticles.

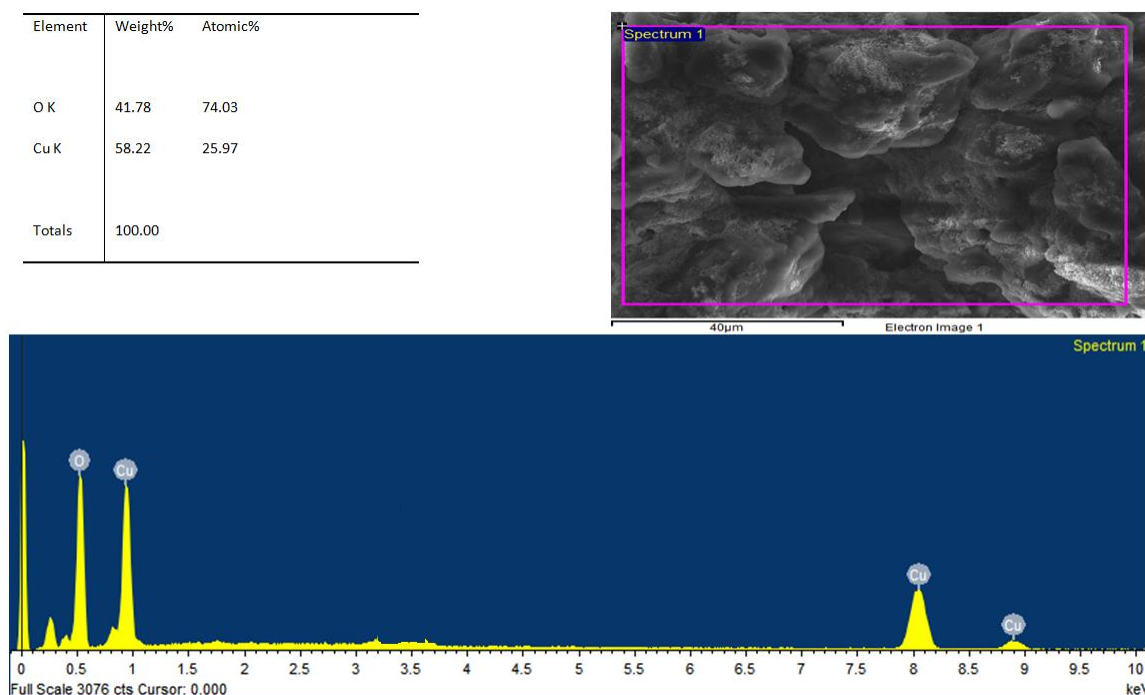


Fig.6.EDX analysis of copper oxide nanoparticles

The dried powder of the sample was analyzed on Energy Dispersive X-ray Analysis (EDX) technique. The peaks have confirmed the presence of copper, oxygen. The average atomic weight percentage ratio of Cu, O. CuO nanoparticle was 58.22: 41.78. The energy ratio (in keV) 25.97: 74.03. The data's are presented in the Fig 6. The presence of doped rare earth element in copper oxide nanoparticles was confirmed by the analysis.

1.3.6. Antimicrobial Screening of copper oxide

The copper oxide nanoparticles are screened in vitro for antibacterial activity against *E. coli*, *B. subtilis* and antifungal activity against *A. niger* by Agar-well diffusion method. The antibacterial and antifungal activities of copper oxide nanoparticles are listed in table.

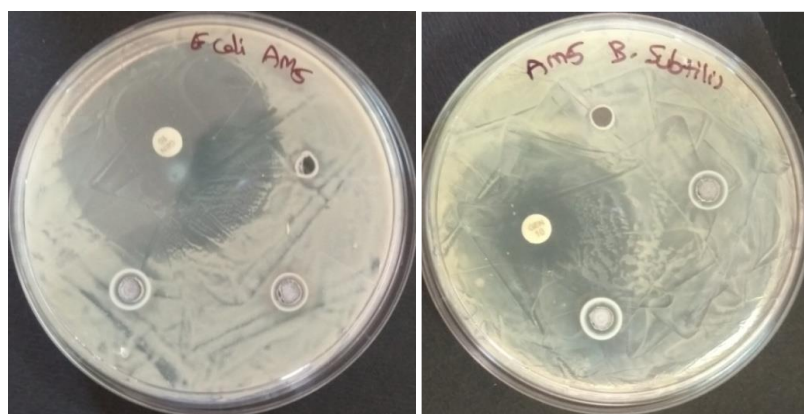


Fig.7. Inhibition zones for CuO against. *B. subtilis* *E. coli*



Fig.8. Inhibition zones for CuO nanoparticles against A. niger

Bacteria	Inhibition zone (mm)
E. coli	08
B. subtilis	08
Fungi	Inhibition zone (mm)
A. Niger	0

Table.3. Antimicrobial activities of copper oxide nanoparticles

The copper oxide nanoparticles showed good antibacterial activity against B. subtilis and E. coli but didn't show anti fungal activity against fungal organisms. We found greater inhibition zones for E.coli and B.subtilis but inhibition zone for A.niger is 0 mm.

1.3.7. Cytotoxic studies of copper oxide nanoparticles

The synthesized CuO nanoparticles are screened for their cytotoxicity (MCF-7, cell lines) [22-54]. From the data, it is observed that the nanoparticles displayed their cytotoxic activities as IC_{50} ($\mu\text{g/mL}$) against breast cancer MCF-7, the IC_{50} value of the nanoparticles are listed in table.4.

Conc($\mu\text{g/ml}$)	% cell survival	% cell inhibition
0.1	89.40216955	10.597830454
1	84.45560466	15.544395339
10	77.47930896	32.52069104
100	24.6870229	75.3129771

Table.4. Dose response of CuO nanoparticles on MCF-7 cell line

The above table illustrated the high potent nature of nanoparticles. The cell survival is decreasing and % of cell inhibition is increasing with the increasing concentration of the nanoparticles compound. The IC_{50} value of the nanoparticles are $44.59(\mu\text{g/mL})$.

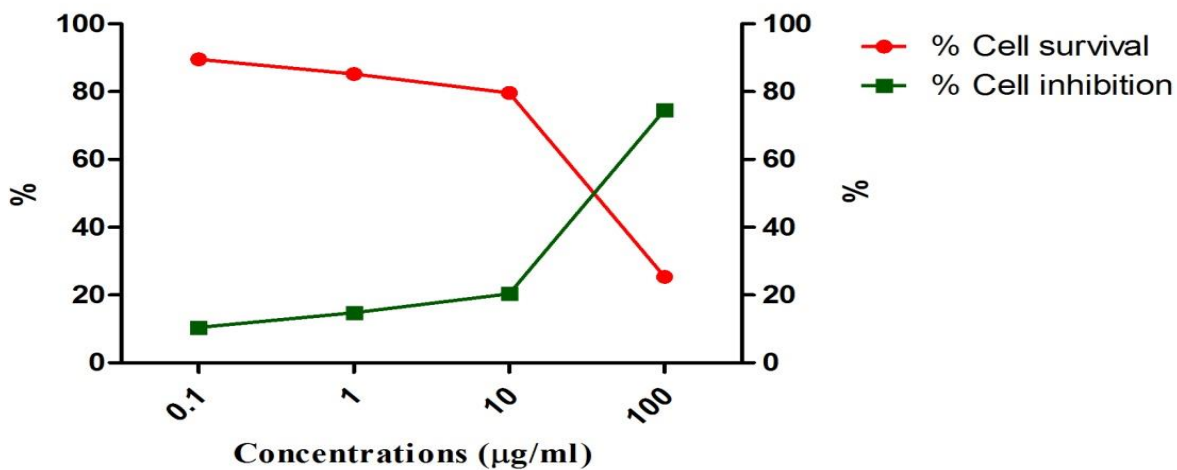


Figure .9. Effect of nanoparticles on MCF-7 Cell Viability for 24 h Incubation time

IC50	44.59µg/mL
-------------	-------------------



1.4. Conclusion

In the present study on “synthesis of copper oxide nanoparticles using chemical method and their antifungal activity”, copper oxide nanoparticles were synthesized using copper nitrate. Synthesis conditions were optimized and resultant nanopowder was characterized using UV- Visible spectroscopy, XRD, FESEM. Morphological analysis report particle size range of 50 nm and also revealed that the nanoparticles are present in the form of aggregates. While studying the effect of copper oxide nanoparticles is screened invitro for antimicrobial activity by disc diffusion method. The bacterial organisms used in this study are E.coli, Bacillus subtilis. The observed inhibition zones for these nanoparticles are in the range of 10-15 mm for E.coli and 10-17 mm for Bacillus subtilis. The screened data in these reports are in good agreement with the previous data and the inhibition zone images are pictorially recorded. This study conclusively reports a synthesis of copper oxide nanoparticles. Such studies have potential for developing good fungicidal formulations having nanoparticles. The cytotoxicity activities of copper oxide nanoparticles screened by MTT assay. We have screened for one type of cancer cell line, viz., MCF-7 (breast cancer), copper oxide obtained IC₅₀ values in the range of 40- 50µg/ml for MCF-7 cell line most of these nanoparticles are in cytotoxic activity. In some cases, the IC₅₀ values are less than the first metal based drug cisplatin.

References

1. S. Lee, U. S. Choi, S. Li and J. A. Eastman, J. Heat Transfer, 121, 280 (1999).
2. K. Borgohain, J. B. Singh, M. V. Rama Rao, T. Shripathi and S. Mahamuni, Phys. Rev., 61, 11093 (2000).
3. E. Darezereshki, F. Bakhtiari, A novel technique to synthesis of tenorite(CuO) nanoparticles from low concentration CuSO₄ solution J. Min. Metal., Sect. B., 47 (2011) 73.
4. G. Yuan, H. Jiang, C. Lin, S. Liao, shape controlled electrochemical synthesis of cupric oxide nanocrystals, J. Cyst. Growth. 303 (2007) 400.
5. Y. Lim, J. Choi, T. Hanrath, Facile synthesis of colloidal CuO nanocrystals for light harvesting applications J. Nanomaterials, 2012 (2012) 4.
6. H. Wang, J. Xu, J. Zhu, , H. Chen, J. Cryst. Growth, 244 (2002) 88.
7. P. Poizot, S. Laruelle, S. Grugeon, L. Dupont, J.M. Tarascon, Nature 407, 496 (2000).
8. V.R. Katti, A.K. Debnath, K.P. Muthe, M. Kaur, A.K. Dusa, S.C. Gadkari., B chem , 245 (2003)
9. H.M. Fan, L.T. Yang, W.S. Hua, X.F. Wu, Z.Y. Wu S.S. Xie, Nano technology. 15, 37 (2004).
10. M.H. Chang, H.S. Liu, C.T. Tai, j. Powder technology 207, 378-386 (2011).
11. C.L. Carnes, K.J. Kalbunde., J. Mol. Catal. A Chem 194, 227-236 (2003).
12. Jose, B.; Ryu, J. H.; Kim, Y. J.; Kim, H.; Kang, Y. S.; Lee, S. D.; Kim, H. S., Chem. Mater. 2002, 14 (5), 2134-2139.
13. Chon, C. H., Kihm, K. D., ASME Journal Heat Transfer, 127 (2005), 8, p. 810
14. Das S. K., et al., , ASME Journal Heat Transfer, 125, (2003), 4, pp. 567-574

15. Nagaraju, M., et al., National Conference on Nano Science, Nano Engineering and Application (NCONSEA-2012), 2012, Kukatpally, Hyderabad, India
16. Aparna, Y., et al., Journal of Nano and Electronic Physics, 4 (2012), 3, pp. 3005-3008
17. Wen, D., Ding, Y., Journal Nanoparticle Res, 7 (2005), 2, pp. 265-274
18. Das, S. K., et al., International Journal of Heat and Mass Transfer, 46 (2003), 5, pp. 851-862
19. Kim, H., et al., Nucl. Eng. Technol., 38 (2006), 1, pp. 61-69
20. Kim, S. J., et al., International Journal of Heat Mass Transfer, 50 (2007), 19-20, pp. 4105-4116
21. Hegde, R. N., et al., Heat and Mass Transfer, 48 (2012), 6, pp. 1031-1041
22. Liu, Z. H., Qiu, Y. H., Journal Heat Mass Transfer, 43 (2007), 7, pp. 699-706
23. [12] Kang, M. G., International Journal Heat Mass Transfer, 43 (2000), 22, pp. 4073-4085
24. Webb, R. L., Pais, C., International Journal of Heat Mass Transfer, 35 (1992), 8, pp. 1893-1904.
25. T.S. Moss, G.J. Burrell and B. Ellis, Butterworth & Co. Ltd, 1973.
26. H.M. Honsi, S.A. Fayek, S.M. El-Sayed, M. Roushdy, M.A. Soliman Vacuum 81, 54 (2006)
27. A. Sawaby, M.S. Selim, S.Y. Marzouk, M.A. Mostafa and A. Hosny, Physica B 405, 3412 (2010).
28. N.F. Mott, E.A. Davies, Electronic Processes in Non-Crystalline Materials (Clarendon Press, Oxford, 1979).
29. A.N. Banerjee and K.K. Chattopadhyay, in D. Depla and S. Maheiu (Eds.), Reactive Sputter Deposition, Springer-Verlag Berlin Heidelberg, 2008, p.465.
30. B.A. Gizhevskii, Y.P. Sukhorukov, A.S. Moskvina, N.N. Loshkareva, E.V. Mostovshchikova, A.E. Ermakov, E.A. Kozlov, M.A. Uimin, V.S. Gaviko, JETP 102, 297(2006).
31. Y.P. Sukhorukov, B.A. Gizhevskii, E.V. Mostovshchikova, A.Y. Yermakov, S.N. Tugushev and E.A. Kozlov, Tech. Phys. Lett. 32, 132 (2006).
32. S.G. Ovchinnikov, B.A. Gizhevskii, Y.P. Sukhorukov, A.E. Ermakov, M.A. Uimin, E.A. Kozlov, Y. Kotov and A.A.V. Bagazeev, Phys. Solid State 49, 1116 (2007).
33. S. Rehman, A. Mumtaz and S.K. Hasanain, Journal of Nanoparticles. Res. 13, 2497 (2011).
34. F.P. Koffyberg and F.A. Benko, Journal of Applied Phys. 53, 1173 (1982).
35. S. Neeleshwar, C.L. Chen, C.B. Tsai, Y.Y. Chen, C.C. Chen, S.G. Shyu and M.S. Seehra, Phys. Rev. B 71, 201307(R) (2005).